

A Convolutional Neural Network-Based Low Complexity Filter

Chao Liu, *Student Member, IEEE* Heming Sun, *Member, IEEE* Jiro Katto, *Member, IEEE*
Xiaoyang Zeng, *Member, IEEE* and Yibo Fan

Abstract—Convolutional Neural Network (CNN)-based filters have achieved significant performance in video artifacts reduction. However, the high complexity of existing methods makes it difficult to be applied in real usage. In this paper, a CNN-based low complexity filter is proposed. We utilize depth separable convolution (DSC) merged with the batch normalization (BN) as the backbone of our proposed CNN-based network. Besides, a weight initialization method is proposed to enhance the training performance. To solve the well known over smoothing problem for the inter frames, a frame-level residual mapping (RM) is presented. We analyze some of the mainstream methods like frame-level and block-level based filters quantitatively and build our CNN-based filter with frame-level control to avoid the extra complexity and artificial boundaries caused by block-level control. In addition, a novel module called RM is designed to restore the distortion from the learned residuals. As a result, we can effectively improve the generalization ability of the learning-based filter and reach an adaptive filtering effect. Moreover, this module is flexible and can be combined with other learning-based filters. The experimental results show that our proposed method achieves significant BD-rate reduction than H.265/HEVC. It achieves about 1.2% BD-rate reduction and 79.1% decrease in FLOPs than VR-CNN. Finally, the measurement on H.266/VVC and ablation studies are also conducted to ensure the effectiveness of the proposed method.

Index Terms—In-loop filter, HEVC, convolutional neural network, VTM.

I. INTRODUCTION

THE performance of video compression has been continuously improved with the development from H.264/AVC [1], H.265/HEVC [2] to H.266/VVC [3]. These standards share a similar hybrid video coding framework, which adopts prediction [4], [5], transformation [6], quantization [7], and

context adaptive binary arithmetic coding (CABAC) [8]. Owing to the modules like quantization and flexible partition, some unavoidable artifacts are produced and cause degradation of video quality, such as blocking effect, Gibbs effect, and ringing. To compensate for those artifacts, many advanced filtering tools are designed, for instance, de-blocking(DB [9]), sample adaptive offset(SAO [10]), and adaptive loop filter(ALF [11]). These tools reduce the artifacts effectively with acceptable complexity.

In the past decades, the learning-based methods make great progress in both low-level and high-level computer vision tasks [12]–[17], such as object detection [12], [13], semantic image segmentation [14], [15], and super resolution [16], [17]. By virtue of the powerful non-linear capability of learning-based tools, they also have been utilized to replace the existing modules in video coding and show great potential, for instance, intra prediction [18]–[20], inter prediction [21], [22], and entropy coding [23], [24]. Learning-based models, especially CNN, have achieved excellent performances for the in-loop filter of video coding [25]–[33]. Dai *et al.* [26], [27] proposed VR-CNN, which adopts a variable filter size technique to have different receptive fields in one-layers and achieves excellent performance with relatively low complexity. Zhang *et al.* [30] proposed a 13-layer RHCNN for both intra and inter frames. The relatively deep network has a strong mapping capability to learn the difference between the original and the reconstructed inter frames. To further adapt to the image content, Jia *et al.* [33] designed a multi-model filtering mechanism and proposed a content-aware CNN with a discriminative network. This method uses the discriminative network to select the most suitable deep learning model for each region.

Most of the learning-based filters can achieve considerable BD-rate [34] savings than H.265/HEVC anchor. However, real-world applications often require lightweight models. High memory usage and computing resource consumption make it difficult to apply complex models to various hardware platforms. Therefore, designing a light network is essential to popularize learning-based in-loop filters. Considering this, some model compression methods that reduce the model complexity while maintaining performance are needed. In recent years, some famous methods have been proposed, including lightweight layers [35], [36], knowledge transfer [37]–[39], low-bit quantization [40], [41], and network pruning [42], [43]. DSC [35], [36] is one of the famous lightweight layers. It preserves the essential features of standard convolution while greatly reducing the complexity by using grouping convolution [35]. In this paper, we build our learning-based filter with DSC

This work was supported in part by the National Natural Science Foundation of China under Grant 61674041, in part by Alibaba Group through Alibaba Innovative Research (AIR) Program, in part by the STCSM under Grant 16XD1400300, in part by the pioneering project of academy for engineering and technology and Fudan-CIOMP joint fund, in part by the National Natural Science Foundation of China under Grant 61525401, in part by the Program of Shanghai Academic/Technology Research Leader under Grant 16XD1400300, in part by the Innovation Program of Shanghai Municipal Education Commission, in part by JST, PRESTO Grant Number JPMJPR19M5, Japan. (Corresponding author: Heming Sun and Yibo Fan.)

C. Liu, Y. Fan and X. Zeng are with the State Key Laboratory of ASIC and System, Fudan University, Shanghai 200433, China (e-mail: chaoliu18@fudan.edu.cn; fanyibo@fudan.edu.cn; xyzeng@fudan.edu.cn).

H. Sun is with the Waseda Research Institute for Science and Engineering, Tokyo 169-8555, Japan and JST, PRESTO, 4-1-8 Honcho, Kawaguchi, Saitama, 332-0012, Japan (e-mail: hemingsun@aoni.waseda.jp).

J. Katto is with Waseda Research Institute for Science and Engineering, Tokyo 169-8555, Japan and the Graduate School of Fundamental Science and Engineering, Waseda University, Tokyo 169-8555, Japan (e-mail: katto@waseda.jp).

instead of the standard convolution. And knowledge transfer is used to help the initialization of the trainable parameters without increasing the complexity.

Besides the learning-based filter itself, we also need a lightweight mechanism for the filtering of inter frames. Some inter blocks fully inherit the texture from their reference blocks and have almost no residuals. If the learning-based filter is used for each frame, those blocks will be repeatedly filtered and cause over-smoothing in inter blocks [33], [44]. One solution to solve this problem is training a specific filter for inter frames [30]. However, the coding of intra and inter frame share some of the same modules in H.265/HEVC like transformation, quantization, and block partitions. This means the learning-based filter trained with intra frames can also be used for inter frames to some extent. Considering this, previous works [27], [33], [44]–[47] designed a syntax element control flag to indicate whether an inter CTU uses the learning-based filter or not. It chooses a selective filtering strategy for each CTU. For this strategy, we compare it with frame-level control in Section IV-A and found the CTU-level control may lead to artificial boundaries between the neighboring CTUs. So we propose to use the frame-level based filter to avoid unnecessary artificial boundaries. In order to improve the performance of frame-level based filtering, we propose a novel module called residual mapping (RM) in this paper.

In summary, we propose a novel light CNN-based in-loop filter for both intra and inter frames based on [48], [49]. Experimental results show this model achieves excellent performance in terms of both video quality and complexity. Specifically, our contributions are as follows.

- A CNN-based lightweight in-loop filter is designed for H.265/HEVC. Low-complexity DSC merged with the BN is used as the backbone of this model. Besides, we use attention transfer to pre-train it to help the initialization of parameters.
- For the filtering of inter frames, we analyze and build our CNN-filter based on frame-level to avoid the artificial boundaries caused by CTU-level. Besides, a novel post-processing module RM is proposed to improve the generalization ability of the frame-level based model and enhance the subjective and objective quality.
- We integrate the proposed method into HEVC and VVC reference software and significant performance has been achieved by our proposed method. Besides, we conduct some extensive experiments like ablation studies to prove the effectiveness of our proposed methods.

The following of this paper is organized as follows. In Section II, we present the related works, including the in-loop filter in video coding and the lightweight network design. Section III elaborates on the proposed network, including network structure and its loss function. Section IV focuses on the proposed RM module and provides an analysis of different control strategies. Experiment results and ablation studies are shown in Section V. In Section VI, we conclude this paper with future work.

II. RELATED WORKS

A. In-loop Filters in Video Coding

1) *DB, SAO, and ALF*: DB, SAO, and ALF that are adopted in the latest video coding standard H.266/VVC [3] are aimed at removing the artifacts in video coding. De-blocking [9] has been used to reduce the discontinuity at block boundaries since the publication of coding standard H.263+ [50]. Depend on the boundary strength and reconstructed average luminance level, DB chooses different coding parameters to filter the distorted boundaries. Meanwhile, by classifying the reconstructed samples into various categories, SAO [10] gives each category a different offset to compensate for the error between the reconstructed and original pixels. Based on the Wiener filter, ALF [11] tries different filter coefficients by minimizing the square error between the original and reconstructed pixels. The signal of the filter coefficient needs to be sent to the decoder side to ensure the consistency between encoder and decoder. All these aforementioned filters can effectively alleviate the various artifacts in reconstructed images. However, there is still much room for improvement.

2) *Learning-based Filter*: Recently, the learning-based filters have far outperformed the DB, SAO, and ALF in terms of both objective and subjective quality. Different from SAO and ALF, they hardly need extra bits but can compensate for errors adaptively as well. Most of them are based on CNNs and have achieved great success in this field. For the filtering of intra frames, Park *et al.* [25] first proposed a CNN-based in-loop filter IFCNN for video coding. Dai *et al.* [26] proposed VR-CNN as post-processing to replace DB and SAO in HEVC. Based on inception, Liu *et al.* [28] proposed a CNN-based filter with 475,233 trainable parameters. Meanwhile, Kang *et al.* [29] proposed a multi-modal/multi-scale neural network with up to 2,298,160 parameters. Considering the coding unit (CU) size information, He *et al.* [31] proposed a partition-masked CNN with a dozen residual blocks. Sun *et al.* [48] proposed a learning-based filter with ResNet [51] for the VTM. Liu *et al.* [49] proposed a lightweight learning-based filter based on DSC. Apart from what was mentioned above, Zhang *et al.* [44] proposed a residual convolution neural network with a recursive mechanism.

Different from the training the filter for intra samples, training the filter with inter samples need to consider the problem of repeated filtering [33], [47]. Jia *et al.* [33] proposed a content-aware CNN based in-loop filtering method that applies multiple CNN models and a discriminative network in the H.265/HEVC. This discriminative network can be used to judge the degree of distortion of the current block and select the most appropriate filter for it. However, the discriminative network requires additional complexity and memory usage, some researchers [27], [45] proposed to use block-level syntax elements to replace it. This method requires extra bit consumption but gets a more accurate judgment on whether to use the learning-based filter. Similarly, some researchers [25], [52] proposed to use frame-level syntax elements to control the filtering of inter frames. Besides, complicated models [30], [45], [53] like spatial-temporal networks are also useful for solving this problem. Jia *et al.* [45] proposed spatial-

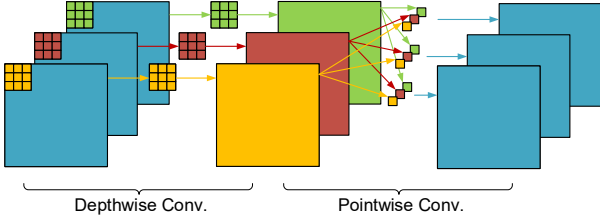


Fig. 1. The depthwise separable convolution, where "Conv." indicates convolution.

temporal residue network (STResNet) with CTU level control to suppress visual artifacts. RHCNN that is trained for both intra and inter frames was proposed by Zhang *et al.* [30]. Filtering in the decoder side [32], [54], [55] can also solve the problem of repeated enhancement well. For example, DS-CNN was designed by Yao *et al.* [32] to achieve quality enhancement as well. Li *et al.* [54] adopted a 20-layers deep CNN to improve the filtering performance. Zhang *et al.* [55] proposed a post-processing network for VTM 4.0.1.

In summary, filtering in inter frames is more challenging than that of intra frames. In most cases, the CNN-based in-loop filter with higher complexity can achieve better performance on intra frames. But for the filtering of inter frames, the existing methods have their own problems. For example, frame-level control may lead to an over-smoothing problem, CTU-level control will cause the additional artificial boundaries, the out-loop filters cannot use the filtered image as a reference, adding discriminative network and complex model may lead to over-complexity and impractical. Therefore, we should pay attention to a more effective method for this task.

B. Lightweight Network Design

1) *Depthwise Separable Convolution*: As a novel neural network layer, DSC achieves great success in practical applications because of its low complexity. It is initially introduced in [35] and subsequently used in MobileNets [36]. As shown in Fig. 1, DSC divides the calculation of standard convolution into two parts, depthwise convolution, and pointwise convolution. Different from standard convolution, depthwise convolution decompose the calculation of standard convolution into group convolution to reduce the complexity. Meanwhile, the pointwise convolution is the same as the standard convolution with kernel 1×1 . In other words, depthwise convolution is used to convolute the separate features whereas pointwise convolution is utilized to combine them to get the output feature maps. These two parts together form a complete DSC.

2) *Knowledge Distillation and Transfer*: Previous studies [37]–[39] have shown that the "knowledge" in pre-trained models can be transferred to another model. Hinton *et al.* [37] propose a distillation method that uses a teacher model to get a "soft target", which helps a student model that has a similar structure perform better in the classification task. Besides softening the target in classification tasks, some other methods [38], [39] use the intermediate representations of the pre-trained model to transfer the "knowledge". For example, Zagoruyko *et al.* [38] devise a method called attention transfer

(AT) to get student model performance improved by letting it mimic the attention maps from a teacher model. Meanwhile, Huang *et al.* [39] design a loss function by minimizing the maximum mean discrepancy (MMD) metric between the distributions of the teacher and the student model, where MMD is a distance metric for probability distributions [56].

III. PROPOSED CNN-BASED FILTER

A. Network Structure

As shown in Fig. 2, we design a network structure that functions on both the teacher and the proposed model. This structure is composed of convolution, BN layer, and activation ReLU [57]. The backbone of this structure is K layers of DSC with dozens of feature maps F . The input to this structure is the HM reconstruction without filtering and the output is the filtered reconstructed samples. The last part is a standard convolution with only 1 feature map. And we add the reconstruction samples to the output inspired by residual learning [51]. The depthwise and the standard convolution kernel are both 3×3 . Every convolution is followed by the ReLU except for the last one. The reason why choose ReLU instead of other advanced activation functions is that ReLU has a lower complexity while a considerable nonlinearity. In our implementation, the values of K and F are 24 and 64 for the teacher model, 9 and 32 for the proposed model. The description of the parameters in the proposed model is shown in Table I.

We use the BN layer in the training phase, this layer could improve the back-propagation of the gradients. What's more, both BN and convolution are linear computations for the tensors in the proposed model. Therefore, the BN can be merged into the convolution to further reduce the computational during the inference phase. As shown in (1), depthwise convolution output χ_{dwConv} can be formulated as:

$$\chi_{dwConv} = w_{dwConv} * \chi \quad (1)$$

where $*$ indicates the convolution operation, w_{dwConv} is the kernel and χ is the depthwise convolution input. Similarly, the piecewise convolution output χ_{pwConv} can be written as:

$$\chi_{pwConv} = w_{pwConv} * \chi_{dwConv} + b_{pwConv} \quad (2)$$

where w_{pwConv} and b_{pwConv} denote the kernel and bias. It is noticeable in (1) that the convolution of depthwise convolution has no bias, this is because the bias b_{dwConv} can be merged into b_{pwConv} when there is no activation between depthwise and pointwise convolution. After convolution, the output of BN can be obtained by (3). (The reason why we use $*$ operation here is because actually the calculation of BN is equivalent to that of the depthwise convolution by simplification)

$$\chi_{bn} = \gamma * \left(\frac{\chi_{pwConv} - \text{mean}}{\sqrt{\text{var} + \epsilon}} \right) + \beta \quad (3)$$

Substituting (2) into (3), we obtain (4) as follows:

$$\chi_{bn} = \hat{w}_{pwConv} * \chi_{dwConv} + \hat{b}_{pwConv} \quad (4)$$

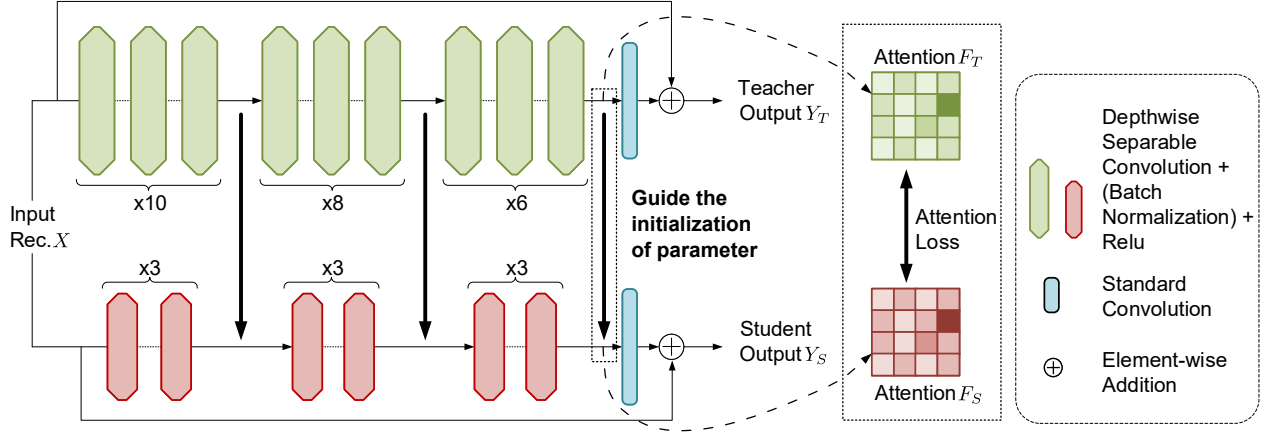


Fig. 2. The architecture of teacher model and the proposed model, where "Rec." indicates "reconstructed pixels". The top-right and bottom-right are the teacher model and the proposed student model, respectively. The rectangle on the right implies the knowledge transfer.

TABLE I
DESCRIPTION OF THE PARAMETERS IN THE PROPOSED MODEL

Index	Block1	Block2	Block3	Std Conv. ^a	Sum
Parameters	73 + 2 × 1,344	3 × 1,344	3 × 1,344	289	11,114

^a Standard Convolution.

where \hat{w}_{pwConv} and \hat{b}_{pwConv} in (4) are:

$$\hat{w}_{pwConv} = \frac{\gamma * w_{pwConv}}{\sqrt{var} + \epsilon} \quad (5)$$

$$\hat{b}_{pwConv} = \frac{\gamma * (b_{pwConv} - mean)}{\sqrt{var} + \epsilon} + \beta \quad (6)$$

In (5) and (6), γ and β are trainable parameters of BN, $mean$ and var are non-trainable parameters of BN. Hyper-parameter ϵ represents a positive number that prevents division zero errors. In the inference phase, we use the \hat{w}_{pwConv} and \hat{b}_{pwConv} to replace the weight w_{pwConv} and bias b_{pwConv} in depthwise convolution, thus merging the BN into the DSC and reducing the model complexity.

B. Standard Convolution of the Proposed Structure

In this subsection, the last part of the proposed structure is detailed. Because the standard convolution uses fewer calculations than DSC when the number of convolution output channels is only one. It is worth noting that the last convolution of the proposed model is standard convolution, which isn't consistent with the backbone of the proposed model. The DSC consists of two steps, including depthwise convolution and pointwise convolution. The depthwise convolution is the simplification of the standard convolution to reduce the amount of computation while preserving the ability to convolve the input feature maps. Meanwhile, the pointwise convolution is equivalent to the standard convolution with 1×1 kernel, it is utilized to fuse the different depthwise convolution output. According to their computing methods, the ratio r of the calculation of the DSC to that of the standard convolution is calculated as:

$$r = \frac{K_W K_H C_I W H + C_I C_O W H}{K_W K_H C_I C_O W H} = \frac{1}{C_O} + \frac{1}{K_W K_H} \quad (7)$$

where W, H is the width and height of the input frame, respectively. K_W, K_H is the width and height of the convolution kernel, respectively. C_I, C_O are the number of feature maps for the convolution input and output, respectively. In our proposed model, $C_O = 1$ and $K_W = 3, K_H = 3$. So $r = \frac{1}{C_O} + \frac{1}{K_W K_H} = \frac{10}{9}$, which is bigger than 1. This represents DSC consumes more computing sources than standard convolution. The extra calculation is caused by pointwise convolution, which is utilized to combine feature maps. However, the standard convolution also can combine features, which indicates the extra calculation of pointwise convolution is meaningless. Therefore, we choose the standard convolution at the end of the model to avoid meaningless calculations.

C. Proposed Initialization and Training Scheme

In this subsection, we will introduce the training process and loss functions of the proposed network. In most cases, a suitable initialization of parameters can help the model better converge to the minimum. Inspired by transfer learning, a pre-trained teacher model is used to guide the initialization of the parameters in the proposed model. By using such initialization, we hope the proposed model can obtain the output similar to that of the teacher model before the real training begins. The pre-trained model uses the mean square errors (MSE) loss between the output Y_T of teacher model and the original pixels Y_O .

$$\mathcal{L}_T = \frac{1}{N} \sum_{i=1}^N \|Y_T^i - Y_O^i\|_2^2 \quad (8)$$

After the training of the teacher model, we use the intermediate outputs of it to guide the proposed model on parameter initialization. This process is denoted by the bold lines in Fig. 2. Because the vanishing of gradients may lead to insufficient training of shallow layers, the teacher model is divided into differently-sized blocks to produce the intermediate hints. The metric of the distance between teacher and the proposed student model tries two forms, including MMD [39] and attention loss [38]. The loss function $\mathcal{L}_{MMD^2}(F_T, F_S)$ with

linear kernel function ($k(x, y) = x^T y$) could be written as follows:

$$\mathcal{L}_{MMD^2}(F_T, F_S) = \left\| \frac{1}{C_T} \sum_{i=1}^{C_T} \frac{f_T^i}{\|f_T^i\|_2} - \frac{1}{C_S} \sum_{j=1}^{C_S} \frac{f_S^j}{\|f_S^j\|_2} \right\|_2^2 \quad (9)$$

where F represents the attention map, f indicates a single feature map, C is the number of feature maps, and the subscript T and S identify the teacher and student model. Meanwhile, the loss function $\mathcal{L}_{AT}(F_T, F_S)$ of attention transfer (AT) [38] could be written as follows:

$$\mathcal{L}_{AT}(F_T, F_S) = \left\| \frac{\sum_{i=1}^{C_T} |f_T^i|^p}{\sum_{i=1}^{C_T} \|f_T^i\|_2^p} - \frac{\sum_{j=1}^{C_S} |f_S^j|^p}{\sum_{j=1}^{C_S} \|f_S^j\|_2^p} \right\|_2^2 \quad (10)$$

We set p to 2 in our implementation, because these two methods are similar except for their normalization methods when $p = 1$ [39]. After the initialization, we start the real training process of using MSE \mathcal{L}_S in (11) to train the proposed model, where Y_S indicates the output of the proposed model.

$$\mathcal{L}_S = \frac{1}{N} \sum_{i=1}^N \|Y_S^i - Y_O^i\|_2^2 \quad (11)$$

In summary, the whole process can be divided into the following steps.

Algorithm 1 The process of building the trained proposed model.

Input: The dataset pair of HM reconstruction samples X and original samples Y_O ;

Output: The trained proposed model;

- 1: Constructing the teacher model T and training it for n_1 epochs with MSE \mathcal{L}_T ;
- 2: Extracting the attention maps F_T from the trained T ;
- 3: Constructing the student model S with BN and training it for n_2 epochs with $\mathcal{L}_{AT}(F_T, F_S)$ or $\mathcal{L}_{MMD^2}(F_T, F_S)$;
- 4: Training S with MSE \mathcal{L}_S for n_3 epochs;
- 5: Calculating the \hat{w}_{pwConv} and \hat{b}_{pwConv} for S ;
- 6: Removing the BN from S ;
- 7: Using the \hat{w}_{pwConv} and \hat{b}_{pwConv} to replace the weight w_{pwConv} and bias b_{pwConv} in depthwise convolution of S ;
- 8: **return** S ;

IV. PROPOSED RESIDUAL MAPPING FOR THE CNN-BASED FILTERING

A. Analysis of CTU-level and Frame-level Control

From the size of filtered samples, filtering methods can be divided into CTU-level (block-level) and frame-level. Compared with CTU-level control, there are two main advantages of frame-level control in CNN-based filter design, including the required computational resource and the video quality. In this subsection, the difference is analyzed from the perspectives of the padding methods and the filter kernels.

Firstly, to keep the input frames size unchanged, the CNN-based filter needs to pad the boundaries of input with some samples. There are usually two padding ways, including

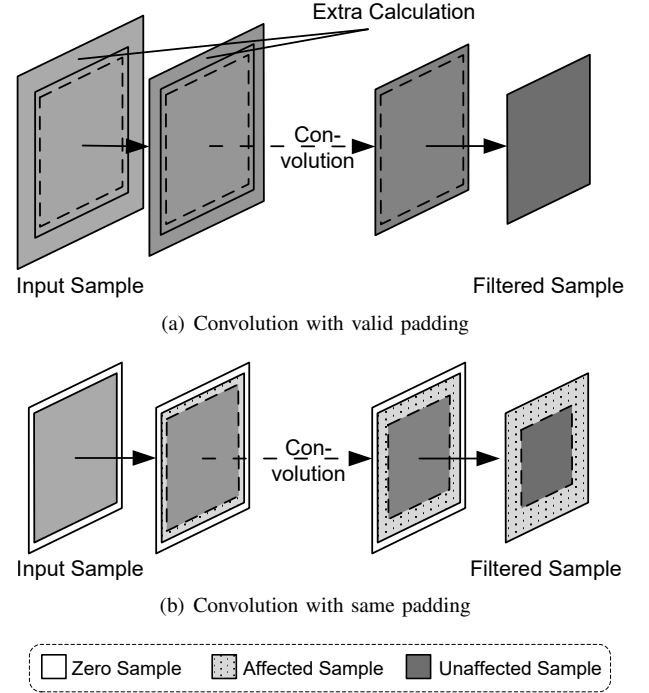


Fig. 3. The diagrams of convolution with different pad methods.

TABLE II
COMPLEXITY COMPARISON OF CTU-LEVEL CONTROL BETWEEN VALID PADDING AND SAME PADDING

Items	RHCNN [30]		Jia <i>et al.</i> [33]		VR-CNN [26]	
Padding type	Valid	Same	Valid	Same	Valid	Same
Flops ^a (G)	16.21	10.89	2.02	1.49	0.25	0.22
Madd ^b (G)	32.38	21.76	4.04	2.97	0.49	0.44
Memory ^c (MB)	91.06	60.11	25.43	18.02	5.84	5.02
MemR+W ^d (MB)	193.05	130.36	55.09	39.42	13.88	11.99

^a Theoretical amount of floating point arithmetics.

^b Theoretical amount of multiply-adds.

^c Memory usage.

^d Memory read /write.

valid padding (padded with reconstructed samples) and same padding (padded with zero samples). In one case, if the CTUs are padded with reconstructed pixels to maintain the same accuracy as frame-level filtering, most of the networks need to pad the input block with plenty of pixels and require considerable calculation. Fig. 3 intuitively shows the difference in the amount of calculation between valid and same padding. The quantitative calculations [58] are illustrated in Table II (we assume that both of their output sizes of filtered samples are 64×64), it can be found that the valid padding (see "Valid" columns) of works [26], [30], [33] all have considerable complexity increasing than same padding (see "Same" columns). In the other case, if the same padding is selected, it will cause calculation errors around the boundaries as shown in Fig. 4. We assume that the size of the block control is $h \times h$, and the width of the boundary area affected by the pad is a . The proportion p_{fc} of affected pixels under frame-control is

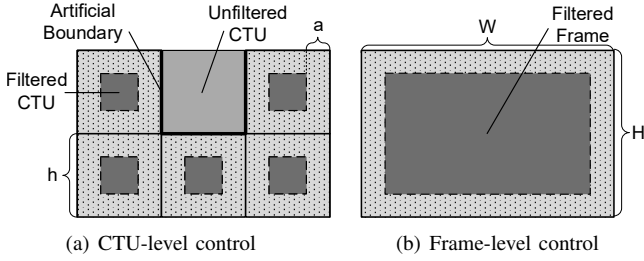


Fig. 4. The diagrams of convolution with different control methods.

calculated as follows:

$$p_{fc} = 1 - \frac{(W - 2a)(H - 2a)}{WH} = \frac{2a(W + H - 2a)}{WH} \quad (12)$$

Similarly, the proportion p_{bc} of affected pixels under block control can be approximated as follows. (No incomplete CTU are considered)

$$p_{bc} = \frac{4a(h - a)}{h^2} \approx \frac{4a}{h} \quad (13)$$

It can be found from (13) that the area affected by same padding is approximately proportional to the perimeter of the filtered samples. Therefore, the frame-level control with a higher area-to-perimeter ratio is less affected than block-level control. According to (12) and (13), it can be obtained that for the HEVC test sequence, the same-padding of our network will affect an average of 45% of the pixels under CTU-level control, whereas that of frame-level control is only 3%. Therefore, choosing frame-level control lays a solid foundation for the application of the CNN-based filter.

Secondly, the frames filtered by frame-level control has the property of integrity. Frame-level control uses the same kernel for filtering of the entire frame whereas CTU-level control may use the different kernels for two consecutive CTUs, which may lead to some artificial errors in the boundaries. As shown in Fig. 4, two consecutive CTUs with different filtering strategies have some errors along the boundaries because of the different kernels used in the filtering. Especially for the condition that one of the CTUs uses the learning-based filter while the other one doesn't. This further demonstrates the advantages of frame-level control.

In summary, for the design of lightweight CNN-based filters, the frame-level control has some advantages over block-level control. On the one hand, compared with frame-level control, CTU-level control leads to calculation cost with the same padding or calculation error with the valid padding. On the other hand, frame-level control has the property of integrity and it brings better subjective quality. To reduce the padding error brought by the multi-layer neural network and complexity, we built our CNN-based in-loop filters on a frame-level control. However, the ability to directly use frame-based control is weak because it only has two states of using or not using the filter, we need some added methods to improve its performance.

B. Residual Mapping

In this subsection, a novel post-processing module RM is proposed to improve the performance of the frame-level

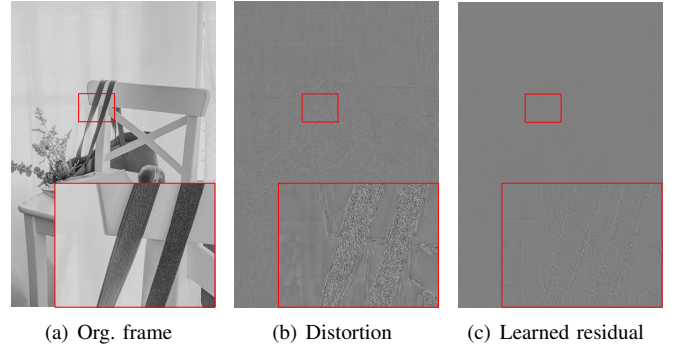


Fig. 5. A frame from CLIC dataset [59] is coded with HM-16.16 and QP 37. The original frame, the distortion and the learned residual of this frame are shown in (a), (b) and (c).

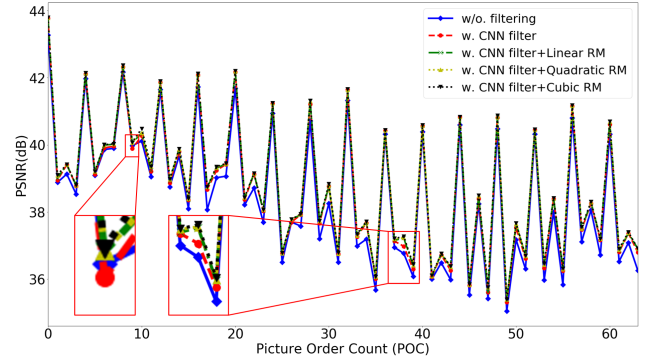


Fig. 6. The comparison of different filtering mechanisms (“Race-Horses_416x240”, qp22, LDP configuration). Linear, quadratic, and cubic represent the mapping function of linear, quadratic, and cubic functions, respectively. We can find in the red box that the performance of using CNN-filter directly is not satisfactory, and even leads to a decrease in PSNR.

control based CNN filter. It can effectively improve the over-smoothing problem [33], [47] of inter frame. Besides, we found that it also has a considerable improvement to intra frames in Section V-D. Most of the trained neural networks are fitting to a certain training set. Since the distribution of training data is often very complicated, the training is actually a trade-off of the data set. For a specific image, the trained filter may be under-fitted or over-fitted. This may cause distortion or blur for a learning-based filter. What's more, if we want to use the neural network trained with intra samples for the filtering of inter samples, this phenomenon will be more serious because of the difference in the distribution of the intra and inter datasets. With this in mind, we proposed to use a parametric RM after the learning-based filter, which is some sort of non-parametric filter, to improve its generalization ability. Inspired by the potential correlation of distortion and learned residual shown in Fig. 5, we handle this filter from the perspective that of restoring distortion from the learning-based filtered residual, which is equivalent to improving the quality of the distorted frames. The distortion R_O is defined as the difference between the original samples Y_O and reconstruction of de-blocking X :

$$R_O = Y_O - X \quad (14)$$

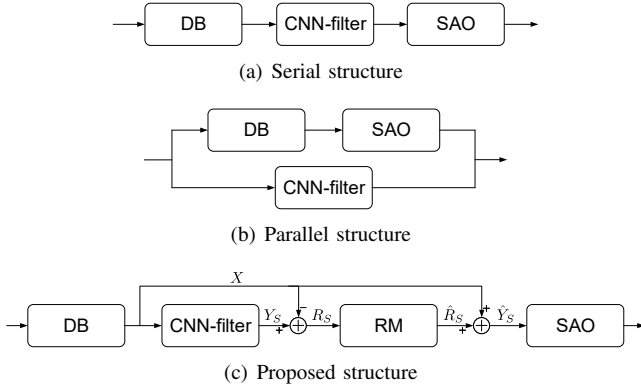


Fig. 7. The schemes of the different frameworks with CNN-based filter.

Similarly, the learned residual R_S is defined as the difference between the output of learning-based filter and X .

$$R_S = Y_S - X \quad (15)$$

A function $f_\lambda(\cdot)$ with parameters λ is designed as the parametric filter to map R_S to R_O . We choose MSE as the metric:

$$\lambda = \arg \min_{\lambda} (f_\lambda(R_S) - R_O)^2 \quad (16)$$

We should use a model with a small amount of parameters to construct $f_\lambda(\cdot)$, so that it is convenient to encode the parameters λ into the bitstream to ensure the consistency of encoding and decoding. For the expression form of $f_\lambda(\cdot)$, we have tried linear functions and polynomial functions as shown in Fig. 6. From the red box on the left, it can be found that only using the CNN filter (see red dotted line) may lead to a decrease in coding performance, this proves that directly using CNN filters for inter frames may degrade video quality. And the performance is improved after adopting RM. It is noticeable that there is little difference in performance between different polynomial functions. So we choose simple linear functions to build RM.

$$\lambda = \arg \min_{\lambda} (\lambda R_S - R_O)^2 \quad (17)$$

So we add X and the output of RM \hat{R}_S to get the filtered frame \hat{Y}_S . After sending it to SAO, the entire filtering process is completed.

$$\hat{Y}_S = X + \hat{R}_S = X + \lambda R_S \quad (18)$$

We quantify the candidate λ with n bits for each component, where $\lambda = i/(2^n - 1)$, $i \in 0, 1, \dots, 2^n - 1$. In the implementation, the number of required bits n is set to 5, so each frame needs 15 bits for the RM module. And a rate-distortion optimization (RDO) process is designed to find the best λ . The regular mode of CABAC is used to code λ . RM does not need specific models for inter frames or additional classifiers for each CTU. What's more, it is independent of the proposed network and can be combined with other learning-based filters to alleviate the over-smoothing problem as well.

Different from previous strategy [47] of choosing one between traditional filtering and learning-based filtering, RM uses a serial structure and makes full use of both these two

TABLE III
EXPERIMENTAL ENVIRONMENT

Items	Specification
Optimizer	Adam [60]
Processor	Intel Xeon Gold 6134 at 3.20 GHz
GPU	NVIDIA GeForce RTX 2080
Operating system	CentOS Linux release 7.6.1810
HM version	16.16
DNN framework	Keras 2.2.4 [61] and TensorFlow 1.12.0 [62]

kinds of filtering as shown in Fig. 7. From the perspective of reconstructed frames, the proposed RM can be interpreted as a post-processing module that fully utilizes the advantages of both distorted reconstruction and learned filtered output. The full use of these two aspects makes RM have excellent performance. For example, we assume that the reference frame is a frame filtered by a learning-based filter, so if the current frame and the reference frame are almost identical, the current frame does not need to use all the filters. Conversely, if the current frame and the reference frame are completely different, it is easy to produce artificial imprints because of the distorted residue, so the filters should be used in this case. For a specific frame, however, it is often difficult to obtain an accurate judgment about whether to use the filters by using its encoded information, such as residuals or motion vectors. Considering the good generalization ability of traditional filters, we keep them working and focused on the CNN filter. So we introduce a parametric module RM, which uses an RDO process to give an appropriate filtering effect of the CNN filter. From (16), it can be observed that the filtering strength varies with the change of the λ . So we can traverse all of the candidate λ and code the one with the smallest reconstruction error into bitstreams. We can also derivative the objective function to obtain the optimal parameters, and code the quantized parameters in the bitstream. In this case, we need to consider the influence of parameter quantization, those mapping functions that are sensitive to quantization noise, such as high-order polynomials, should be abandoned. Otherwise, this may result in larger quantization errors in the decoded frames.

V. EXPERIMENTAL RESULTS

A. Experimental Setting

For the experiment, we mainly focus on objective quality, subjective quality, complexity, and ablation studies to illustrate the performance of our model. Nine hundred pictures from DIV2K [63] are cropped into the resolution of 1024×1024 , and then down-sampled to 512×512 . These two sets of pictures are spliced into two videos as our training sets. Only the luminance component is used for training, and the chrominance components are also tested by using the proposed model. The patch size in training is 32×32 of H.265/HEVC and 64×64 of H.266/VVC, which is consistent with the largest size of the TU. Considering that the reconstructed images with different QPs often have different degrees of

distortion and artifacts, the whole QP band is divided into four parts, below 24, 25 to 29, 30 to 34, and above 35. So four proprietary models are trained for each QP band. The parameter initialization method is normal distribution [64] for both the teacher model and the proposed model. The training epochs n_1 and n_3 are both set to 50. We use more training epochs for the model with higher QP in the special initialization phase because there are often more artifacts in the reconstructed images with higher QP. Specifically, parameters n_2 is set as 10 for the lower QPs and 20 for the higher QPs. After the training phase, we save the trained model and call it to infer in HEVC reference software (HM) and video coding test model (VTM). In the test phase, the first 64 frames from HEVC test sequences are used to evaluate the generalization ability of our model. We test four different configurations with default settings, including all-intra (AI), low-delay-B (LDB), low-delay-P (LDP), and random-access (RA) for H.265/HEVC anchor. For the H.266/VVC anchor, we test it with default AI and RA configurations. Four typical QPs in common test conditions are tested, including 22, 27, 32, 37. The other important test conditions are shown in Table III. For a fair comparison with previous works, we use the coding experimental results from their original papers. The complexities of the reference papers are tested on our local server to avoid the influence of the hardware platforms.

B. Experiment on H.265/HEVC

1) *Objective Evaluation*: In this subsection, the objective evaluation is conducted to evaluate the performance of our proposed model. The experimental results compared with the HM-16.16 anchor are shown in Table IV. For the luminance component, the proposed model achieves 6.3%, 4.5%, 5.4%, and 5.7% BD-rate reduction compared with HEVC baseline under AI, LDB, LDP, and RA configuration, respectively. For chrominance components, the proposed model achieves more BD-rate reduction than the luminance component. It demonstrates the generalization ability for the proposed model because we only use the luminance components of intra samples for training. Furthermore, the comparisons with the previous works [26], [33] are conducted and the BD-rate reduction is shown in Table V. It can be seen that our model achieves more BD-rate reduction for AI configuration.

For the performance evaluation of inter configurations, we introduce the comparison of our proposed model with frame-level control [25], CTU-level control [45], and Jia *et al.* [33] as shown in Table VI. To compare fairly, we select the same padding and use the proposed model to test the different control methods. From the experiment results, it can be seen that our proposed model achieves about 1% extra BD-rate reduction than both CTU-level and frame-level control for all inter configurations. Compared with Jia *et al.* [33], our model achieves comparative BD-rate reduction in inter configurations. For the chrominance components, our model achieves about 3% extra BD-rate reduction, it further demonstrates the generalization ability of our model.

2) *Subjective Evaluation*: We also conduct the subjective evaluation as shown in Fig. 8 and Fig. 9. It can be seen

from the experimental results that our model has a great de-artifacts capability. First, we re-deploy the proposed model in HM-16.9 for a fair subjective evaluation with Jia *et al.* [33]. From Fig. 8, it can be found that the various kinds of artifacts in (a) are eliminated by the proposed model and the man's face looks smoother and plump. At the same time, some vertical blocky effects are produced by Jia *et al.* [33], probably because it uses different filters for consecutive CTUs while our proposed model uses the same filter for the whole images and have no additional boundaries. Besides, the man's eyes seem to be blurred by [33] and lead to the degradation of visual quality. Second, the subjective evaluation for the inter frames is conducted in Fig. 9. The default HM and HM with CTU-level control [27] are used as the anchors. As shown in Fig. 9, the contouring and blocky artifacts on the number are eliminated by the proposed model. For CTU-level control [27] based filtering, the subjective quality of this frame is reduced due to the artificial boundaries on the knee, whereas our proposed model has no boundaries on it and achieves a better visual quality. To sum up, because our proposed method makes full use of the frame-level filtering strategy, the proposed method has significantly better visual effects than previous CTU-based methods.

3) *Complexity Analysis*: As shown in Table V, we compare the complexity of Jia *et al.* [33], VR-CNN [26], and our proposed model from two aspects, including computational complexity and storage consumption. Firstly, for the coding complexity evaluation, we use the following equation to calculate the ΔT :

$$\Delta T = \frac{T'}{T} \quad (19)$$

where T' and T denote the HM coding time with and without the learning-based filter, respectively. FLOPs in Table V are also tested for the frame with a resolution of 720p. Compared with VR-CNN [26], the FLOPs of our model is reduced by 79.1%. The decoding complexity is reduced by approximately 50% and the encoding complexity is reduced by 4%. The processing time of the proposed model is almost the same for both encoder and decoder. The difference in relative time is caused by that the network inference time accounts for a small proportion of the encoding complexity but comparative for the decoding.

In terms of storage consumption, compared with [26], the number of trainable parameters in the proposed model is reduced by 79.6%. It is almost the same with the reduction of model size because we use the same precision (float32) to save the models. The main reason why our model has relatively fewer parameters is that the design of the proposed model focuses more on complexity instead of performance. For example, we use the DSC as the backbone of the proposed model, whereas previous works [26], [33] utilize the standard convolution. Meanwhile, we also use many useful methods to limit the model size while maintaining the performance, including BN merge and special initialization of parameters. What's more, our proposed model only needs one learning-based network for both intra and inter frames. So there is no need for additional models in practical applications. Compared with previous works that need multiple models or

TABLE IV
BD-RATE REDUCTION OF THE PROPOSED METHOD THAN HM-16.16 ANCHOR

Sequences		AI			LDB			LDP			RA		
		Y	U	V	Y	U	V	Y	U	V	Y	U	V
ClassA	Traffic	-7.3%	-3.4%	-4.7%	-4.6%	-2.4%	-0.9%	-4.3%	-3.4%	-1.5%	-6.4%	-3.6%	-2.7%
	PeopleOnStreet	-6.8%	-7.1%	-6.9%	-4.5%	-0.6%	-0.9%	-3.1%	-4.4%	-2.4%	-6.1%	-4.6%	-5.0%
ClassB	Kimono	-4.9%	-2.6%	-2.5%	-4.6%	-7.5%	-4.7%	-7.3%	-11.5%	-6.7%	-4.2%	-5.7%	-3.4%
	ParkScene	-5.5%	-3.2%	-2.3%	-1.9%	-0.3%	-0.7%	-1.5%	-0.5%	-0.7%	-3.8%	-0.6%	-0.3%
	Cactus	-5.3%	-4.1%	-10.1%	-4.4%	-3.7%	-4.4%	-5.4%	-5.6%	-5.8%	-6.8%	-9.5%	-7.2%
	BasketballDrive	-4.3%	-8.9%	-11.7%	-3.4%	-4.2%	-7.8%	-6.0%	-9.2%	-11.7%	-4.4%	-4.4%	-8.9%
	BQTerrace	-3.7%	-4.3%	-4.8%	-6.1%	-2.1%	-2.4%	-10.6%	-4.5%	-3.9%	-8.8%	-3.8%	-3.3%
ClassC	BasketballDrill	-8.0%	-11.7%	-14.1%	-2.8%	-4.9%	-4.6%	-3.4%	-5.6%	-6.2%	-4.2%	-8.0%	-9.7%
	BQMall	-6.0%	-6.3%	-7.2%	-3.8%	-3.2%	-4.7%	-4.6%	-4.5%	-5.6%	-5.1%	-4.7%	-5.1%
	PartyScene	-3.7%	-4.8%	-5.7%	-0.8%	-0.1%	-0.2%	-1.8%	-0.4%	-0.4%	-1.7%	-1.4%	-2.0%
	RaceHorses	-3.9%	-6.9%	-12.0%	-4.1%	-6.6%	-11.3%	-4.2%	-7.9%	-12.7%	-4.7%	-9.7%	-14.2%
ClassD	BasketballPass	-6.5%	-7.3%	-10.3%	-4.4%	-3.3%	-4.6%	-4.3%	-4.8%	-5.8%	-3.9%	-4.7%	-6.1%
	BQSquare	-4.2%	-3.0%	-6.8%	-2.4%	-1.6%	-2.8%	-4.1%	-1.8%	-2.9%	-2.4%	-1.0%	-2.9%
	BlowingBubbles	-5.3%	-9.3%	-9.8%	-3.6%	-5.8%	-2.1%	-3.9%	-5.4%	-1.8%	-4.0%	-6.1%	-4.4%
	RaceHorses	-7.5%	-10.5%	-14.6%	-6.3%	-5.2%	-10.3%	-6.7%	-7.4%	-10.8%	-6.8%	-9.4%	-12.2%
ClassE	Vidyo1	-8.9%	-8.7%	-10.5%	-6.7%	-9.0%	-9.6%	-7.4%	-9.4%	-8.9%	-8.1%	-8.4%	-9.7%
	Vidyo3	-7.0%	-5.2%	-5.3%	-4.0%	-5.9%	-3.1%	-4.6%	-6.3%	-2.5%	-6.5%	-4.1%	-5.1%
	Vidyo4	-6.3%	-10.1%	-10.8%	-3.8%	-11.5%	-10.9%	-3.9%	-12.1%	-11.2%	-5.6%	-9.8%	-10.1%
	FourPeople	-9.4%	-8.1%	-9.0%	-8.6%	-9.2%	-9.4%	-9.0%	-9.7%	-10.8%	-9.4%	-7.7%	-8.1%
	Johnny	-8.3%	-12.3%	-11.0%	-7.0%	-11.4%	-9.1%	-9.6%	-13.1%	-10.7%	-8.3%	-10.9%	-9.7%
	KristenAndSara	-8.6%	-10.2%	-11.1%	-7.7%	-8.3%	-8.6%	-8.3%	-10.1%	-11.2%	-8.2%	-8.9%	-9.6%
Average		-6.3%	-7.0%	-8.6%	-4.5%	-5.1%	-5.4%	-5.4%	-6.6%	-6.4%	-5.7%	-6.1%	-6.6%

TABLE V
BD-RATE REDUCTION AND COMPLEXITY (GPU) OF THE PROPOSED METHOD COMPARED WITH PREVIOUS WORKS [26], [33] IN AI CONFIGURATION

Sequences	Jia et al. [33]					VR-CNN [26]					Proposed model				
	Y	U	V	ΔT_{enc}	ΔT_{dec}	Y	U	V	ΔT_{enc}	ΔT_{dec}	Y	U	V	ΔT_{enc}	ΔT_{dec}
ClassA	-4.7%	-3.3%	-2.6%	108.1%	734.9%	-5.5%	-4.7%	-4.9%	108.3%	561.1%	-7.1%	-5.4%	-5.9%	105.8%	281.0%
ClassB	-3.5%	-2.8%	-3.0%	109.0%	659.8%	-3.3%	-3.2%	-3.7%	110.3%	505.3%	-4.8%	-4.8%	-6.4%	106.2%	265.2%
ClassC	-3.4%	-3.5%	-5.0%	113.1%	894.9%	-5.0%	-5.5%	-6.9%	113.0%	685.1%	-5.4%	-7.5%	-9.9%	106.5%	326.3%
ClassD	-3.2%	-4.7%	-6.0%	128.9%	1406.0%	-5.4%	-6.4%	-8.1%	121.6%	1047.1%	-5.9%	-7.8%	-10.5%	114.4%	548.0%
ClassE	-5.8%	-4.1%	-5.2%	112.3%	1110.2%	-6.5%	-5.5%	-5.6%	111.1%	836.7%	-8.1%	-9.2%	-9.7%	107.2%	401.1%
Average	-4.1%	-3.7%	-4.4%	114.3%	961.2%	-5.1%	-5.1%	-5.8%	112.9%	727.0%	-6.3%	-7.0%	-8.6%	108.0%	364.3%
FLOPs	334.84G					50.39G					10.51G				
Parameters	362,753					54,512					11,114				
Model size	1.38MB					220KB					58KB				

TABLE VI
OVERALL BD-RATE COMPARISON OF PREVIOUS METHODS [25], [33], [45] IN LDB, LDP, AND RA CONFIGURATION

Methods	LDB			LDP			RA		
	Y	U	V	Y	U	V	Y	U	V
Jia et al. [33]	-6.0%	-2.9%	-3.5%	-4.7%	-1.0%	-1.2%	-6.0%	-3.2%	-3.8%
Our network + RM	-4.5%	-5.1%	-5.4%	-5.4%	-6.6%	-6.4%	-5.7%	-6.1%	-6.6%
Our network + Frame control [25]	-3.7%	-3.3%	-3.2%	-4.4%	-4.6%	-3.9%	-4.6%	-4.8%	-5.1%
Our network + CTU control [45]	-4.1%	-4.4%	-4.9%	-4.6%	-5.8%	-5.9%	-4.5%	-5.1%	-5.8%

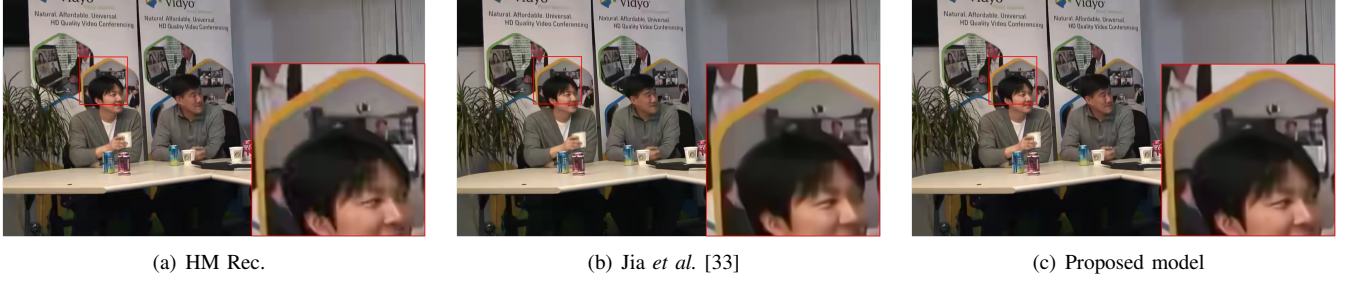


Fig. 8. Visual quality comparison of Jia *et al.* [33] and the proposed model for AI configuration. The test qp is 37 and this is the 1st frame for FourPeople(Anchor HM-16.9).

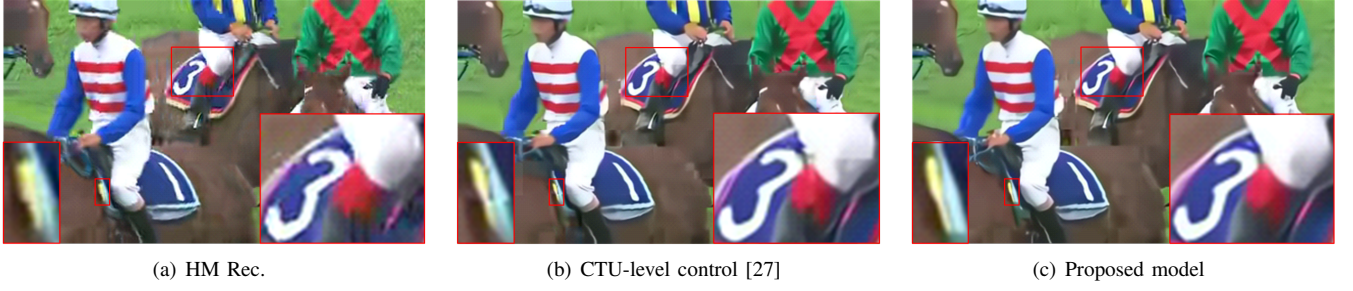


Fig. 9. Visual quality comparison of CTU-level control [27] and the proposed model for RA configuration. The test QP is 37 and this is the 16th frame for RaceHorse(Anchor HM-16.16).

TABLE VII
BD-RATE REDUCTION AND COMPUTATIONAL COMPLEXITY (GPU) OF THE PROPOSED METHOD THAN VTM-6.3 ANCHOR

Sequences		AI					RA				
		Y	U	V	ΔT_{enc}	ΔT_{dec}	Y	U	V	ΔT_{enc}	ΔT_{dec}
ClassA	Traffic	-1.6%	-0.2%	-0.4%	100.7%	234.1%	-1.1%	-0.7%	-0.5%	99.6%	357.0%
	PeopleOnStreet	-1.3%	-0.4%	-0.3%	98.0%	225.4%	-0.9%	-0.1%	-0.2%	99.7%	266.3%
ClassB	Kimono	-0.3%	0.1%	-0.3%	104.9%	317.5%	-0.2%	0.0%	-0.4%	99.8%	319.3%
	ParkScene	-1.9%	0.1%	-0.1%	108.3%	232.4%	-1.4%	0.3%	-0.2%	101.2%	302.1%
	Cactus	-1.3%	-0.5%	-0.8%	100.4%	244.5%	-1.4%	-1.8%	-1.7%	103.1%	343.9%
	BasketballDrive	-0.3%	-0.8%	-1.0%	103.7%	282.7%	-0.4%	-0.8%	-0.5%	100.5%	321.0%
	BQTerrace	-1.0%	-0.6%	-0.6%	101.6%	228.4%	-1.9%	-1.6%	-1.5%	101.6%	313.0%
	BasketballDrill	-2.7%	-3.8%	-5.5%	101.6%	219.2%	-1.6%	-3.4%	-2.9%	102.9%	270.8%
ClassC	BQMall	-2.2%	-0.8%	-0.7%	100.4%	220.6%	-2.0%	-1.1%	-0.5%	104.6%	285.1%
	PartyScene	-1.8%	-1.1%	-1.5%	100.5%	198.7%	-1.3%	-1.6%	-1.8%	101.7%	242.7%
	RaceHorses	-0.9%	-1.1%	-2.3%	101.6%	233.5%	-1.1%	-1.5%	-2.5%	99.5%	243.8%
	BasketballPass	-2.1%	-1.4%	-4.7%	99.4%	407.5%	-1.2%	-2.4%	-1.0%	98.0%	406.1%
ClassD	BQSquare	-3.0%	-0.2%	-1.0%	103.0%	319.1%	-3.6%	-1.0%	-1.6%	105.6%	421.0%
	BlowingBubbles	-2.1%	-1.4%	-1.0%	101.1%	352.0%	-1.6%	-2.3%	-2.4%	101.0%	371.1%
	RaceHorses	-2.8%	-2.7%	-4.6%	99.6%	366.6%	-2.4%	-3.1%	-6.5%	98.6%	312.1%
ClassE	Vidyo1	-1.3%	-0.1%	-0.3%	101.5%	340.3%	-1.0%	-0.1%	0.4%	102.6%	486.6%
	Vidyo3	-1.1%	0.2%	-0.2%	101.8%	298.8%	-1.2%	1.5%	0.9%	102.0%	457.4%
	Vidyo4	-0.8%	-0.3%	-0.2%	106.4%	291.0%	-1.0%	0.3%	-1.4%	101.3%	425.5%
	FourPeople	-2.1%	-0.5%	-0.5%	99.2%	263.3%	-1.8%	-0.8%	-0.7%	106.2%	449.3%
	Johnny	-1.3%	-0.4%	-0.6%	99.9%	317.9%	-2.6%	-1.2%	-1.1%	100.1%	452.4%
	KristenAndSara	-1.7%	-0.6%	-0.7%	101.1%	344.5%	-1.6%	-0.4%	-1.4%	100.2%	428.0%
Average		-1.6%	-0.8%	-1.3%	101.6%	282.8%	-1.5%	-1.0%	-1.3%	101.4%	355.9%

TABLE VIII
ABLATION STUDY OF RM (AI, VTM-6.3)

Sequences	Our network			Our network+RM		
	Y	U	V	Y	U	V
ClassA	-0.5%	-0.1%	0.4%	-1.5%	-0.3%	-0.4%
ClassB	0.3%	1.3%	0.1%	-1.0%	-0.3%	-0.5%
ClassC	-1.6%	-1.8%	-2.8%	-1.9%	-1.7%	-2.5%
ClassD	-2.6%	-2.2%	-3.6%	-2.5%	-1.4%	-2.8%
ClassE	-0.3%	2.6%	1.5%	-1.4%	-0.3%	-0.4%
Average	-0.9%	0.3%	-0.7%	-1.6%	-0.8%	-1.3%

TABLE IX
ABLATION STUDY OF PARAMETER INITIALIZATION (AI, VTM-6.3)

Methods	Δ PSNR(dB)		
	Y	U	V
Student	0.310	0.231	0.295
Student + MMD [39]	0.320	0.245	0.313
Student + AT [38]	0.329	0.256	0.328

classifiers, our proposed method reduces the required storage consumption effectively benefit from the RM module.

C. Experiment on H.266/VVC

To further evaluate the performance of our proposed model, we use the same test condition to test its performance in VTM-6.3. The only difference is that we use the entire DIV2k instead of the down-sampled dataset to train the proposed model. From the experimental results shown in Table VII, it can be found that our model achieves about 1.6% and 1.5% BD-rate reduction on the luminance component for AI and RA configurations. For chrominance components, it also achieved similar performance on BD-rate reduction. In terms of complexity, the proposed method introduces a negligible increase on the encoding side and brings about 3 times complexity to the decoding side.

D. Ablation Study

1) *RM for intra frames*: RM can effectively improve the generalization ability of learning-based filters. The experiments of RM about the inter frames have been carried out in Section V-B. Based on VTM here, we further conduct ablation experiments on intra frames to illustrate the performance of RM. Its test setting is the same as before. From the experiment shown in Table VIII, we can find about 0.8% BD-rate reduction has been achieved by the RM module. Regarding the performance of class-B, only using the proposed CNN-filter may even have a negative effect and leads to 0.3% BD-rate increment. But its performance has been well improved after using RM. For most other classes, the performance has also been improved more or less after using RM.

2) *The initialization of parameters*: The 1-st frame of all HEVC test sequences is tested and the overall PSNR increments are shown in Table IX, where the student model

without transfer learning is indicated as "Student" row. MMD and AT in Table IX represent different transfer learning ways that act on the student model. By comparing the "Student" row with the other rows, we can find that the PSNR of the student model is improved by both MMD and AT. What's more, the improvements of the chrominance components are more obvious than that of the luminance component.

VI. CONCLUSION

In this paper, a CNN-based low complexity filter is proposed for video coding. The lightweight DSC merged with the batch normalization is used as the backbone. Based on the transfer learning, attention transfer is utilized to initialize the parameters of the proposed network. By adding a novel parametric module RM after the CNN filter, the generality of the CNN filter is improved and can also handle the filtering problem of inter frames. What's more, RM is independent of the proposed network and can also combine with other learning-based filters to alleviate the over-smoothing problem. The experimental results show our proposed model achieves excellent performance in terms of both BD-rate and complexity. For HEVC test sequences, our proposed model achieves about 1.2% BD-rate reduction and 79.1% FLOPs than VR-CNN anchor. Compared with Jia *et al.* [33], our model achieves comparative BD-rate reduction with much lower complexity. Finally, we also conduct the experiments on H.266/VVC and ablation studies to demonstrate the effectiveness of the model. Our future work aims at further performance improvement of the learning-based filter in video coding.

REFERENCES

- [1] T. Wiegand, G. J. Sullivan, G. Bjontegaard, and A. Luthra, "Overview of the h. 264/avc video coding standard," *IEEE Transactions on circuits and systems for video technology*, vol. 13, no. 7, pp. 560–576, 2003.
- [2] G. J. Sullivan, J.-R. Ohm, W.-J. Han, and T. Wiegand, "Overview of the high efficiency video coding (hevc) standard," *IEEE Transactions on circuits and systems for video technology*, vol. 22, no. 12, pp. 1649–1668, 2012.
- [3] H266. <https://de.wikipedia.org/wiki/h.266/>, 2018. 4.
- [4] J. Lainema, F. Bossen, W.-J. Han, J. Min, and K. Ugur, "Intra coding of the hevc standard," *IEEE Transactions on Circuits and Systems for Video Technology*, vol. 22, no. 12, pp. 1792–1801, 2012.
- [5] J.-L. Lin, Y.-W. Chen, Y.-W. Huang, and S.-M. Lei, "Motion vector coding in the hevc standard," *IEEE Journal of selected topics in Signal Processing*, vol. 7, no. 6, pp. 957–968, 2013.
- [6] T. Nguyen, P. Helle, M. Winken, B. Bross, D. Marpe, H. Schwarz, and T. Wiegand, "Transform coding techniques in hevc," *IEEE Journal of Selected Topics in Signal Processing*, vol. 7, no. 6, pp. 978–989, 2013.
- [7] O. Crave, B. Pesquet-Popescu, and C. Guillemot, "Robust video coding based on multiple description scalar quantization with side information," *IEEE Transactions on Circuits and Systems for Video Technology*, vol. 20, no. 6, pp. 769–779, 2010.
- [8] D. Marpe, H. Schwarz, and T. Wiegand, "Context-based adaptive binary arithmetic coding in the h. 264/avc video compression standard," *IEEE Transactions on circuits and systems for video technology*, vol. 13, no. 7, pp. 620–636, 2003.
- [9] A. Norkin, G. Bjontegaard, A. Fuldseth, M. Narroschke, M. Ikeda, K. Andersson, M. Zhou, and G. Van der Auwera, "Hevc deblocking filter," *IEEE Transactions on Circuits and Systems for Video Technology*, vol. 22, no. 12, pp. 1746–1754, 2012.
- [10] C.-M. Fu, E. Alshina, A. Alshin, Y.-W. Huang, C.-Y. Chen, C.-Y. Tsai, C.-W. Hsu, S.-M. Lei, J.-H. Park, and W.-J. Han, "Sample adaptive offset in the hevc standard," *IEEE Transactions on Circuits and Systems for Video technology*, vol. 22, no. 12, pp. 1755–1764, 2012.

- [11] C.-Y. Tsai, C.-Y. Chen, T. Yamakage, I. S. Chong, Y.-W. Huang, C.-M. Fu, T. Itoh, T. Watanabe, T. Chujoh, M. Karczewicz et al., "Adaptive loop filtering for video coding," *IEEE Journal of Selected Topics in Signal Processing*, vol. 7, no. 6, pp. 934–945, 2013.
- [12] K. Duan, S. Bai, L. Xie, H. Qi, Q. Huang, and Q. Tian, "Centernet: Keypoint triplets for object detection," in *Proceedings of the IEEE International Conference on Computer Vision*, 2019, pp. 6569–6578.
- [13] Z.-Q. Zhao, P. Zheng, S.-t. Xu, and X. Wu, "Object detection with deep learning: A review," *IEEE transactions on neural networks and learning systems*, 2019.
- [14] X. Liu, Z. Deng, and Y. Yang, "Recent progress in semantic image segmentation," *Artificial Intelligence Review*, vol. 52, no. 2, pp. 1089–1106, 2019.
- [15] C. Liu, L.-C. Chen, F. Schroff, H. Adam, W. Hua, A. L. Yuille, and L. Fei-Fei, "Auto-deeplab: Hierarchical neural architecture search for semantic image segmentation," in *Proceedings of the IEEE Conference on Computer Vision and Pattern Recognition*, 2019, pp. 82–92.
- [16] X. Hu, H. Mu, X. Zhang, Z. Wang, T. Tan, and J. Sun, "Meta-sr: A magnification-arbitrary network for super-resolution," in *Proceedings of the IEEE Conference on Computer Vision and Pattern Recognition*, 2019, pp. 1575–1584.
- [17] J. W. Soh, G. Y. Park, J. Jo, and N. I. Cho, "Natural and realistic single image super-resolution with explicit natural manifold discrimination," in *Proceedings of the IEEE Conference on Computer Vision and Pattern Recognition*, 2019, pp. 8122–8131.
- [18] J. Li, B. Li, J. Xu, R. Xiong, and W. Gao, "Fully connected network-based intra prediction for image coding," *IEEE Transactions on Image Processing*, vol. 27, no. 7, pp. 3236–3247, 2018.
- [19] Y. Hu, W. Yang, M. Li, and J. Liu, "Progressive spatial recurrent neural network for intra prediction," *IEEE Transactions on Multimedia*, vol. 21, no. 12, pp. 3024–3037, 2019.
- [20] H. Sun, Z. Cheng, M. Takeuchi, and J. Katto, "Enhanced intra prediction for video coding by using multiple neural networks," *IEEE Transactions on Multimedia*, 2020.
- [21] J. Liu, S. Xia, W. Yang, M. Li, and D. Liu, "One-for-all: Grouped variation network-based fractional interpolation in video coding," *IEEE Transactions on Image Processing*, vol. 28, no. 5, pp. 2140–2151, 2018.
- [22] L. Zhao, S. Wang, X. Zhang, S. Wang, S. Ma, and W. Gao, "Enhanced motion-compensated video coding with deep virtual reference frame generation," *IEEE Transactions on Image Processing*, 2019.
- [23] R. Song, D. Liu, H. Li, and F. Wu, "Neural network-based arithmetic coding of intra prediction modes in hevc," in *2017 IEEE Visual Communications and Image Processing (VCIP)*. IEEE, 2017, pp. 1–4.
- [24] C. Ma, D. Liu, X. Peng, Z.-J. Zha, and F. Wu, "Neural network-based arithmetic coding for inter prediction information in hevc," in *2019 IEEE International Symposium on Circuits and Systems (ISCAS)*. IEEE, 2019, pp. 1–5.
- [25] W. Park and M. Kim, "Cnn-based in-loop filtering for coding efficiency improvement," in *2016 IEEE 12th Image, Video, and Multidimensional Signal Processing Workshop (IVMSP)*, July 2016, pp. 1–5.
- [26] Y. Dai, D. Liu, and F. Wu, "A convolutional neural network approach for post-processing in hevc intra coding," in *International Conference on Multimedia Modeling*. Springer, 2017, pp. 28–39.
- [27] Y. Dai, D. Liu, Z.-J. Zha, and F. Wu, "A cnn-based in-loop filter with cu classification for hevc," in *2018 IEEE Visual Communications and Image Processing (VCIP)*. IEEE, 2018, pp. 1–4.
- [28] C. Liu, H. Sun, J. Chen, Z. Cheng, M. Takeuchi, J. Katto, X. Zeng, and Y. Fan, "Dual learning-based video coding with inception dense blocks," in *2019 Picture Coding Symposium (PCS)*, Nov 2019, pp. 1–5.
- [29] J. Kang, S. Kim, and K. M. Lee, "Multi-modal/multi-scale convolutional neural network based in-loop filter design for next generation video codec," in *2017 IEEE International Conference on Image Processing (ICIP)*, Sep. 2017, pp. 26–30.
- [30] Y. Zhang, T. Shen, X. Ji, Y. Zhang, R. Xiong, and Q. Dai, "Residual highway convolutional neural networks for in-loop filtering in hevc," *IEEE Transactions on Image Processing*, vol. 27, no. 8, pp. 3827–3841, Aug 2018.
- [31] X. He, Q. Hu, X. Zhang, C. Zhang, W. Lin, and X. Han, "Enhancing hevc compressed videos with a partition-masked convolutional neural network," in *2018 25th IEEE International Conference on Image Processing (ICIP)*, Oct 2018, pp. 216–220.
- [32] R. Yang, M. Xu, and Z. Wang, "Decoder-side hevc quality enhancement with scalable convolutional neural network," in *2017 IEEE International Conference on Multimedia and Expo (ICME)*. IEEE, 2017, pp. 817–822.
- [33] C. Jia, S. Wang, X. Zhang, S. Wang, J. Liu, S. Pu, and S. Ma, "Content-aware convolutional neural network for in-loop filtering in high efficiency video coding," *IEEE Transactions on Image Processing*, vol. 28, no. 7, pp. 3343–3356, 2019.
- [34] G. Bjontegard, "Calculation of average psnr differences between rd-curves," *VCEG-M33*, 2001.
- [35] L. Sifre and S. Mallat, "Rigid-motion scattering for image classification, 2014," Ph.D. dissertation, Ph. D. thesis, 2014.
- [36] A. G. Howard, M. Zhu, B. Chen, D. Kalenichenko, W. Wang, T. Weyand, M. Andreetto, and H. Adam, "Mobilenets: Efficient convolutional neural networks for mobile vision applications," *arXiv preprint arXiv:1704.04861*, 2017.
- [37] G. Hinton, O. Vinyals, and J. Dean, "Distilling the knowledge in a neural network," *Computer Science*, vol. 14, no. 7, pp. 38–39, 2015.
- [38] S. Zagoruyko and N. Komodakis, "Paying more attention to attention: Improving the performance of convolutional neural networks via attention transfer," *arXiv preprint arXiv:1612.03928*, 2016.
- [39] Z. Huang and N. Wang, "Like what you like: Knowledge distill via neuron selectivity transfer," *arXiv preprint arXiv:1707.01219*, 2017.
- [40] J. Yang, X. Shen, J. Xing, X. Tian, H. Li, B. Deng, J. Huang, and X.-s. Hua, "Quantization networks," in *Proceedings of the IEEE Conference on Computer Vision and Pattern Recognition*, 2019, pp. 7308–7316.
- [41] M. Nagel, M. van Baalen, T. Blankevoort, and M. Welling, "Data-free quantization through weight equalization and bias correction," *arXiv preprint arXiv:1906.04721*, 2019.
- [42] P. Molchanov, A. Mallya, S. Tyree, I. Frosio, and J. Kautz, "Importance estimation for neural network pruning," in *Proceedings of the IEEE Conference on Computer Vision and Pattern Recognition*, 2019, pp. 11 264–11 272.
- [43] C. Zhao, B. Ni, J. Zhang, Q. Zhao, W. Zhang, and Q. Tian, "Variational convolutional neural network pruning," in *Proceedings of the IEEE Conference on Computer Vision and Pattern Recognition*, 2019, pp. 2780–2789.
- [44] S. Zhang, Z. Fan, N. Ling, and M. Jiang, "Recursive residual convolutional neural network-based in-loop filtering for intra frames," *IEEE Transactions on Circuits and Systems for Video Technology*, vol. 30, no. 7, pp. 1888–1900, 2020.
- [45] C. Jia, S. Wang, X. Zhang, S. Wang, and S. Ma, "Spatial-temporal residue network based in-loop filter for video coding," in *2017 IEEE Visual Communications and Image Processing (VCIP)*, Dec 2017, pp. 1–4.
- [46] J. Yao, X. Song, S. Fang, and L. Wang, "Ahg9: Convolutional neural network filter for inter frame," Apr 2018, jVET-J0043.
- [47] D. Ding, L. Kong, G. Chen, Z. Liu, and Y. Fang, "A switchable deep learning approach for in-loop filtering in video coding," *IEEE Transactions on Circuits and Systems for Video Technology*, vol. 30, no. 7, pp. 1871–1887, 2020.
- [48] H. Sun, C. Liu, J. Katto, and Y. Fan, "An image compression framework with learning-based filter," in *Proceedings of the IEEE/CVF Conference on Computer Vision and Pattern Recognition Workshops*, 2020, pp. 152–153.
- [49] C. Liu, H. Sun, J. Katto, X. Zeng, and Y. Fan, "A learning-based low complexity in-loop filter for video coding," in *2020 IEEE International Conference on Multimedia & Expo Workshops (ICMEW)*. IEEE, 2020, pp. 1–6.
- [50] G. Cote, B. Erol, M. Gallant, and F. Kossentini, "H. 263+: Video coding at low bit rates," *IEEE Transactions on circuits and systems for video technology*, vol. 8, no. 7, pp. 849–866, 1998.
- [51] K. He, X. Zhang, S. Ren, and J. Sun, "Deep residual learning for image recognition," in *Proceedings of the IEEE conference on computer vision and pattern recognition*, 2016, pp. 770–778.
- [52] Y. Wang, H. Zhu, Y. Li, Z. Chen, and S. Liu, "Dense residual convolutional neural network based in-loop filter for hevc," in *2018 IEEE Visual Communications and Image Processing (VCIP)*. IEEE, 2018, pp. 1–4.
- [53] J. W. Soh, J. Park, Y. Kim, B. Ahn, H.-S. Lee, Y.-S. Moon, and N. I. Cho, "Reduction of video compression artifacts based on deep temporal networks," *IEEE Access*, vol. 6, pp. 63 094–63 106, 2018.
- [54] C. Li, L. Song, R. Xie, and W. Zhang, "Cnn based post-processing to improve hevc," in *2017 IEEE International Conference on Image Processing (ICIP)*. IEEE, 2017, pp. 4577–4580.
- [55] F. Zhang, C. Feng, and D. R. Bull, "Enhancing vvc through cnn-based post-processing," in *2020 IEEE International Conference on Multimedia and Expo (ICME)*. IEEE, 2020, pp. 1–6.
- [56] A. Gretton, K. M. Borgwardt, M. J. Rasch, B. Schölkopf, and A. Smola, "A kernel two-sample test," *Journal of Machine Learning Research*, vol. 13, no. Mar, pp. 723–773, 2012.
- [57] V. Nair and G. E. Hinton, "Rectified linear units improve restricted boltzmann machines," in *Proceedings of the 27th international conference on machine learning (ICML-10)*, 2010, pp. 807–814.

- [58] <https://github.com/Lyken17/pytorch-OpCounter>.
- [59] Workshop and Challenge on Learned Image Compression. 2020. [Online]. <http://www.compression.cc/challenge>.
- [60] D. P. Kingma and J. Ba, "Adam: A method for stochastic optimization," *arXiv preprint arXiv:1412.6980*, 2014.
- [61] F. Chollet *et al.*, "Keras," <https://github.com/fchollet/keras>, 2015.
- [62] M. Abadi, A. Agarwal, P. Barham, E. Brevdo, Z. Chen, C. Citro, G. S. Corrado, A. Davis, J. Dean, M. Devin, S. Ghemawat, I. Goodfellow, A. Harp, G. Irving, M. Isard, Y. Jia, R. Jozefowicz, L. Kaiser, M. Kudlur, J. Levenberg, D. Mané, R. Monga, S. Moore, D. Murray, C. Olah, M. Schuster, J. Shlens, B. Steiner, I. Sutskever, K. Talwar, P. Tucker, V. Vanhoucke, V. Vasudevan, F. Viégas, O. Vinyals, P. Warden, M. Wattenberg, M. Wicke, Y. Yu, and X. Zheng, "TensorFlow: Large-scale machine learning on heterogeneous systems," 2015, software available from tensorflow.org. [Online]. Available: <http://tensorflow.org/>
- [63] E. Agustsson and R. Timofte, "Ntire 2017 challenge on single image super-resolution: Dataset and study," in *The IEEE Conference on Computer Vision and Pattern Recognition (CVPR) Workshops*, July 2017.
- [64] K. He, X. Zhang, S. Ren, and J. Sun, "Delving deep into rectifiers: Surpassing human-level performance on imagenet classification," in *Proceedings of the IEEE international conference on computer vision*, 2015, pp. 1026–1034.